REVEALING THE EFFECTS OF CERIUM DIOXIDE NANOPARTICLES THROUGH THE ANALYSIS OF MORPHOLOGICAL CHANGES IN CHIRONOMUS RIPARIUS

Dimitrija Savić-Zdravković[a]*, Djuradj Milošević[a], Jelena Conić[a], Katarina Marković[b,c], Janez Ščančar[b,c], Marko Miliša[d], Boris Jovanović[e`]

[a] Faculty of Science and Mathematics, University of Niš, Višegradska 33, 18000 Niš, Serbia

[b] Department of Environmental Sciences, Jožef Stefan Institute, Jamova 39, 1000 Ljubljana, Slovenia

[c] Jožef Stefan International Postgraduate School, Jamova 39, 1000 Ljubljana, Slovenia

[d] Department of Biology, Faculty of Science, University of Zagreb, Rooseveltov trg 6, 10000 Zagreb, Croatia

[e] Department of Ecology, Evolution, and Organismal Biology, Iowa State University, Ames, Iowa, USA

*corresponding author. e-mail: dimitrija.savic@pmf.edu.rs; phone number: +38166428090; personal postal address: Stanoja Bunuševca 10, 18000 Niš, Serbia

e-mail addresses of all authors (in consecutive order): dimitrija.savic@pmf.edu.rs; djuradj.milosevic@pmf.edu.rs; jelena.conic@pmf.edu.rs; katarina.markovic@ijs.si; janez.scancar@ijs.si; marko.milisa@biol.pmf.hr; nanoaquatox@gmail.com

ABSTRACT

Due to their many practical applications, engineered cerium dioxide (CeO_2) nanoparticles (NPs) are commonly used today, although there are justified concerns about the environmental risks of their usage. Studies to date have shown that CeO_2 NPs do not pose a lethal hazard to hydrobiocenoses at environmentally relevant concentrations, but that they induce significant negative sublethal effects. Therefore, intensive work is being done on the adaptation of standard ecotoxicological tests with the development of new, sublethal biomarkers. The present study

aims to examine the sublethal effects of prolonged exposure to CeO_2 NPs (2.5; 25; 250 and 2500 mg of CeO_2 NPs per 1 kg of sediment) on the morphological features of the non-biting aquatic midge *Chironomus riparius*. Morphological variation was examined by means of two approaches: (1) Deformity rate analysis (analysis of visible morphological malformations) and (2) Geometric morphometric analysis (analysis of differences in the size and shape of the larval mandibles and mentums, as well as adult male and female wings). Changes in all the morphological structures examined were observed using a geometric morphometric approach at low and very high concentrations of CeO_2 NPs (2.5 and 2500 mg of CeO_2 NPs per 1 kg of sediment). The potential reduction of sexual dimorphism resulting from downsizing of the wings in females was observed. These results indicate that the sublethal changes observed in chironomids exposed to CeO_2 NPs are significant and may potentially lead to further changes in metabolism, diet and behavior, which may lead to repercussions of as yet unexamined proportions. Considering our findings, and the advantages of geometric morphometrics (precision, uniformity, accurate qualification, quantification, and visualization of fine morphological changes), this approach is proven to be an exceptional assessment tool, with great applicative potential in the ecotoxicological testing of nanoparticles.

KEYWORDS

Cerium dioxide; *Chironomus riparius*; Geometric morphometrics; OECD protocols; Metal oxide nanoparticles

1 INTRODUCTION

The presence of engineered nanoparticles (NPs) in the environment seems inevitable, due to the growing number of nanoproducts (Roco, 2003; Boxall et al., 2008), and so there are justified concerns about the environmental risks of nanotechnology. Hornyak et al. (2018) point out that nanotechnology could lead to a new industrial revolution because of the tremendous benefits and positive aspects it brings with it. Great progress has been made in the field of nanotoxicology and ecotoxicology testing; nevertheless, regulatory agencies have not yet made a decision on whether NPs should be treated as a separate class of pollutants (Lead et al., 2018; Hund-Rinke et al., 2016). Considering the production volume of metal oxide nanoparticles, the most relevant nanoparticles for ecotoxicological studies are TiO_2, CeO_2, FeOx, AlO and ZnO (Bundschuh et al., 2018). Due to their many practical applications, particularly in electronics, optics, catalysis, coating and paint production, CeO_2 NPs are commonly used in nanomaterials today (Tella et al., 2015). It is estimated that the world production of CeO_2 NPs is up to 10,000 tons per year (Piccinno et al., 2012; Collin et al., 2014), of which as many as 3240 tons are used only in Europe (Wang and Nowack, 2018). The predicted environmental concentration of CeO_2 in freshwater is 7 ng/L (mode value), while in the freshwater sediment the concentration is 49 µg/kg (assuming 100% degradation after one year), or 901 µg/kg (assuming zero degradation of nanoparticles) (Giese at al., 2018). Similar concentrations of CeO_2 have been estimated across vast freshwater regions of Europe, with an estimated concentration of 2 ng/L for surface freshwater and 35 µg/kg for freshwater sediments (Wang and Nowack, 2018).

Natural fresh groundwater and surface water are the ultimate recipients of toxic substances used for industrial, agricultural, and generally anthropogenic activities (Anderson and

D'Apollonia, 1978). A meta-analysis conducted in 2014 showed that a large number of CeO_2 NP analyses had been performed on freshwater biota (only a small number of species were tested, in several taxonomic groups, mostly daphnids), however, analyses on benthic organisms, even though extremely relevant, were almost completely absent (Collin et al., 2014). Most previous studies have concluded that NPs, in concentrations found in nature, cannot cause lethal effects in laboratory studies, but can have sublethal effects (Bayat et al., 2015; Lee et al., 2009), such as genotoxicity (Lee et al., 2009; Bour et al., 2015), disruption of lysosome systems (Garaud et al., 2015) or inhibition of different cell functions (Artells et al., 2013; Rodea-Palomares et al., 2011). The responses of organisms represent an early warning of the presence of stressors, before the impact reaches dramatic proportions and leads to lethal consequences. Accordingly, it is advisable to develop appropriate methods for assessing the impact of NPs based on sublethal parameters as early indicators of environmental pollution.

The development of ecotoxicology in the last decade includes intensive work on biomarker research and the adaptation of standard ecotoxicological tests for the examination of newly formed chemical agents (OECD, 2019; 2004). Evaluation of the morphological variability of different model organisms has been used as biomarker that can indicate the presence of environmental stress (Cvetković et al., 2020; Savić-Zdravković et al., 2018; Hoffmann et al., 2005). Analyses of the morphology of organisms are the basis of many biological studies in the fields of systematics, taxonomy and evolution. Shape, according to the formal definition, is the geometry of an object when its position, orientation and size are taken away (Kendall, 1977), and as such is ideal for quantitative analysis. The basic "tool" in the analysis of changes in morphological units is morphometry - data obtained by measurements are analyzed using

statistical methods to investigate the shape and size of morphological objects, and to investigate the relationship between morphology and external and internal factors (Rohlf, 1990). These analyses can determine whether there is any influence of an external stressor on the phenotype (shape and size of morphological structures) and then quantify that influence. In geometric morphometry, the objects that are analyzed are defined mathematically through the configuration of specific delineated points describing their geometry, after which they are analyzed by statistical methods that investigate the difference in their shape, and the differences between objects are visualized by direct graphical representation methods (Rohlf, 1990). Although the method of geometric morphometry was developed for the needs of taxonomic research, since it is possible to monitor fine and subtle changes in structures using computer software, it shows great potential for application in ecotoxicology (Arambourou et al., 2012; Cvetković et al., 2020; Stanković et al., 2020; Savić-Zdravković et al., 2018). Chironomids, which are standard model organisms in ecotoxicological tests (OECD, 2020), exhibit morphological changes due to the presence of environmental stressors (Martinez et al., 2002; Di Veroli et al., 2014), and individuals of deformed phenotypes have been found in sediments contaminated with organic and inorganic substances, especially heavy metals (Al-Shami et al., 2011; Servia et al., 2004; Martinez et al., 2002; Tomilina et al., 2020; 2015). Hamilton and Saether (1971) were the first to propose the use of chironomid larval deformities to indicate water quality, and Warwick and Tisdale (1988) were the first to examine larvae (Chironomus, Cryptochironomus, and Procladius) in more detail and illustrate typical deformities on the head structures of chironomid larvae. In his doctoral dissertation, Gagliardi (2017) cites a total of 142 studies (published in the form of scientific papers, chapters, and books) that use chironomid deformities

in the interpretation of ecotoxicity (laboratory and field analyses). The already mentioned method of geometric morphometry was first used in assessing the influence of chemical agents on chironomids in a study by Arambourou et al. (2012), in which it proved to be an extremely sensitive and very objective approach to ecotoxicological analysis.

In previous research on CeO_2 NP toxicity to the sediment dwelling freshwater midge, *Chironomus riparius* (Savić-Zdravković et al., 2020), we confirmed the ingestion of CeO_2 NPs by the larvae and observed significant negative effects at the DNA level, therefore the aim of the present research is to further investigate the sensitivity of additional biological markers adequate for NP assessment. Continuing the work from our previous research, the present study aims to examine the effects of prolonged exposure to CeO_2 NPs on the larval and adult morphological features of the aquatic midge, *C. riparius*, through further specific goals:

(1) to assess the phenotypic effects of CeO_2 NP treatments on chironomid larvae by examining any visible morphological malformations of the larval mouthparts (deformity rate analysis);

(2) to assess the phenotypic effects of CeO_2 NP treatments on chironomid larvae and adults by examining variations in the size and shape of the mouthparts, and male and female wings, using a geometric morphometric approach;

(3) to examine the sensitivity of these methods (deformity rate and geometric morphometric analysis) and their potential in nanoparticle ecotoxicological assessment.

2. MATERIALS AND METHODS

2.1 Tested substance: Cerium oxide nanoparticles (CeO_2 NPs)

Cerium oxide nanoparticles (CeO_2 NPs) were purchased from Sigma-Aldrich in the form of commercially available ceria nanopowder (polycrystalline sample). Detailed characterization of the batch used was conducted in our previous study (Savić-Zdravković et al., 2020), and it will be only briefly described here. Transmission electron microscopic imaging revealed a particle size of between 23 and 29 nm, with an average size of 25 ± 1.8 nm. X-ray diffraction measurements showed the face-centered cubic fluorite crystal structure of the NPs, whilst X-ray photoelectron spectroscopy showed sharply defined peaks characteristic for CeO_2, with their surface partially covered with hydroxide OH groups, and a cerium-to-oxygen ratio typical for a fluorite crystal structure. Brunauer–Emmett–Teller analysis revealed a surface area of 42.6 $m^2 g^{-1}$, pore volume of 1.172 cc g^{-1} and pore radius of 1075.761 Å. The average hydrodynamic radius was calculated as 671 ± 112 nm, with polydispersity in a range from 0.879 to 0.655 and a zeta potential of 28 mV, indicating moderate NP stability in deionized water. Detailed analysis of the morphology, state of aggregation, and particle size of the CeO_2 NPs in the experimental sediment medium for the chironomids revealed the CeO_2 NP aggregate's tendency to cling to silicon dioxide (SiO_2) sand particles. This analysis also revealed that the typical size distribution of CeO_2 NP aggregates adsorbed to the sediment was 2-25 μm.

2.2 Model organism: *Chironomus riparius*

Larvae and adults of the non-biting midge *C. riparius* (Diptera, Chironomidae) were used as a model organism in the present study. The specimens of *C. riparius* were taken from the stock culture at the laboratory of the Faculty of Science and Mathematics, University of Niš (Niš,

Serbia). The stock culture was reared in glass tanks under the Organisation for Economic Co-operation and Development (OECD, 2004) guidelines, which include a water temperature of 23 ± 2 °C; a 16:8 h light/dark photoperiod (neon lamps 1000 lux); constant aeration; and feeding the larvae with finely ground TetraMin fish food. The water medium consisted of a mixture of tap and deionized water with pH 7.6 and total hardness of 350 mg l^{-1} $CaCO_3$. For the stock culture sediment, shredded cellulose paper was used, prepared as proposed by Batac-Catalan and White (1982). New specimens from natural populations were added to the stock culture every few months to maintain genetic stability.

2.3 Experimental procedure

All specimens collected for geometric morphometric analysis originated from the previously completed study (Savić-Zdravković et al., 2020). In brief, *C. riparius* specimens were exposed to increasing concentrations of CeO_2 NPs in the sediment, according to OECD test guideline 218 "Sediment-water chironomid toxicity test using spiked sediment" (OECD, 2004).

2.3.1 Sediment spiking and experimental setup

Chironomid larvae were exposed to sediment spiked with four concentrations of CeO_2 NPs, i.e., NP treatments: 2.5; 25; 250 and 2500 mg of CeO_2 NPs per 1 kg of sediment and a control, each in 4 replicas. The CeO_2 NP treatments were determined in our previous paper (Savić-Zdravković et al., 2020) according to the maximum estimated environmental concentrations for freshwater sediments in Europe (Gottschalk et al., 2015; Wang and Nowack, 2018).

The substrate used in the experiment consisted exclusively of quartz sand (particles between 0.05 and 0.2 mm in size), which was thoroughly washed with distilled water and

incubated in a dry heat sterilizer (VimS Electric SSW 120, Serbia) at 180 °C for 180 minutes, for sterilization before use. To spike the sediment, the following procedure was applied: a solution with an appropriate concentration of CeO_2 NPs in distilled water was prepared, then added directly to the substrate and mixed thoroughly by hand (for 10 minutes daily, repeated for three days) to distribute the nanoparticles as evenly as possible. The sediment prepared in this way was added to the test vessels, i.e., replicas (glass beakers, V = 600 ml, d = 8 cm) in a 3 cm deep layer, then overlaid with water (deionized : tap water, 1:1, pH 7 ± 0.5; hardness 7.0 °dH; conductivity 326 mS cm^{-3}). The test vessels were placed in an isothermal room (23 ± 1°C; 16:8 h light : dark daily cycle). After 3 days, *C. riparius* specimens were added to the test vessels.

The control vessels were prepared in the same way, but without the addition of CeO_2 NPs to the sediment.

2.3.2 Model organism exposure

One freshly laid large egg mass from the stock culture was collected with a blunt pipette and placed in a Petri dish filled with water from the stock culture aquaria. The larvae hatched after 2 days, and twenty-five of them were added to each replica when 4 days old (still at the 1^{st} instar). All of the larvae originated from one egg mass (to obtain genetic uniformity). After 24 h, gentle aeration was provided for each replica through a plastic pipette fixed 2 cm above the sediment layer. The chironomids were fed with finely ground TetraMin fish food every second day (0.5 mg per larva for the first 2 days, and 1 mg per larva for the rest of the experiment).

The complete experimental setup was repeated twice, in order to analyze a series of morphological endpoints on both larval and adult specimens. The first experiment was terminated on the 27^{th} day, 5 days after the emergence of the last adult in the control (adult

midge flies were collected from each replica for further analysis). The second experiment was terminated on the 10th day, 3 days after the first 4th instar larvae were noticed (4th instar larvae were collected from each replica for further analysis).

2.4 Morphological variation analysis

Upon the termination of the experiment, all specimens collected were preserved in 95% EtOH for a short period before preparation for further analysis. The morphological variation was examined using two approaches:

(1) Deformity rate analysis (visual analysis of visible morphological malformations) was carried out to determine the differences in deformity rate in specimens treated with CeO_2 NPs and to test the sensitivity of the method.

(2) Geometric morphometric analysis was performed to determine the differences in size and shape of specimens treated with CeO_2 NPs and to test the sensitivity of the method.

The mouthparts in the larvae, i.e., right mandibles (Figure 1a), and mentums (Figure 1b), and the adult body structures, i.e., male and female right wings (Figure 1c) were investigated.

2.4.1 Sample preparation

The larval specimens (a total of 275 individuals) were dissected in distilled water and prepared for microscope slide mounting, i.e., their head capsules were removed and cooked at 100 °C in 15% KOH for 15 min to soften the mentums and mandibles and, thus, enhance the mounting. The head capsules were then mounted on microscope slides using Berlese's medium (homemade) in a ventral-view position in order to observe the mentums, whilst the right mandibles were removed and mounted separately in lateral position. The microscope slides

were left to dry for 20 days, after which they were examined and photographed under a microscope, the mentums at 100 x and the mandibles at 200 x magnification (Leica MZ16A stereomicroscope with 10 x / 21B ocular and 10 x and 20 x objective magnification and Leica DFC320 Digital Camera system).

The adult specimens (a total of 75 female, and 75 male individuals) were dissected in distilled water and prepared for microscope slide mounting, i.e., their right wings were detached and mounted on microscope slides using Berlese's medium in a lateral position. The mounted wings were overlaid with an additional layer of Berlese's medium after 10 days of drying and were then examined and photographed under a microscope, at 10x magnification (Nikon stereoscopic microscope SMZ 745T, with CeW 10 x B / 22 Nikon objective and 1 x ocular magnification). To investigate the differences in phenotypic response to CeO_2 NP exposure between sexes, the male and female wings were analyzed separately.

2.4.2 Deformity rate analysis

Photomicrographs of all the structures were first examined visually to assess the influence of CeO_2 NPs on any visible morphological malformations of the larval mouthparts (deformity rate). Structures were considered as deformed if obvious deviations from their normal appearance were noticed (extra tooth, missing tooth, or fusing teeth). If visible damage and missing teeth with a rough surface were noticed, the structures were not considered deformed, but broken or damaged.

The following parameters were assessed: (1) visible morphological malformations; (2) visible structural wear.

2.4.3 Geometric morphometric analysis

Secondly, photomicrographs of all the structures were examined using the method of geometric morphometrics to assess the influence of CeO_2 NPs on variations in the size and shape of larval and adult morphological structures. Out of the total number of photomicrographs, structures with severe deformations, wear or accidental damage caused by mounting were excluded from further geometric morphometric analysis. Specimens with "extreme" values were also excluded by MorphoJ software, using the "outlier" function (Klingenberg, 2011). The number of structures analyzed was distributed relatively evenly among the groups.

The following parameters were assessed: (1) variation in the size and shape of the mouthparts (right mandibles and mentum); (2) variation in the size and shape of the wings (right male and female wings).

To describe, explore and quantify the variations in size and shape of the structures, a set of specific landmarks (LMs) was digitized on each structure using two available programs: MakeFun6 (Sheets, 2003) and tpsDig2 (Rohlf, 2005). A total of 18 LMs were digitized on each observed mandible, 29 on each observed mentum and 13 on each wing. Digitized LMs describe the following structures of the mandibles (Figure 1a): 1 and 2 - apical tooth; 2 to 8 - three inner teeth; 9 to 18 - distal outer line of the mandible. For the mentums, which have object symmetry, the LMs are positioned in the following way (Figure 1b): 1 to 8 - four small lateral teeth on the left side of the mentum; 22 to 28 - four small lateral teeth on the right side; 8 to 12 - two larger inner lateral teeth on the left side; 18 to 22 - two larger inner lateral teeth on the right side; 12 to 18 - trifid median tooth. For the wings, the LMs are positioned to describe longitudinal and cross-veins (Figure 1c): 1 and 2 - humeral cross-vein; 3 and 4 - anal vein; 5 and 6 - cubital vein; 7 -

distal end of the medial vein; 8 and 9 - distal ends of radial veins; 10 - end of the subcostal vein; 11 - costal vein; 12 and 13 - radio-medial cross-vein. For more details on the methodology see Savić-Zdravković et al. (2018).

Before further geometric morphometric analysis, statistical tests were conducted using the Statistica data analysis software system, version 7 (StatSoft, 2004). Variation in size (estimated as the centroid size for each constellation of selected landmarks among the analyzed traits - CS) was statistically tested with the analysis of variance (ANOVA), whilst the variation in shape was tested with multivariate analysis of variance (MANOVA), performed on the full set of shape variables. Pairwise comparisons between the groups were conducted using Tukey's *post hoc* test (with significance set at $p < 0.05$).

All further geometric morphometric analysis was conducted using MorphoJ, an integrated software package for geometric morphometrics (Klingenberg, 2011). Individuals were grouped into five groups, based on CeO_2 NP treatments as a classifier: 2.5; 25; 250 and 2500 mg kg^{-1} NP treatments and a control group.

To eliminate differences in orientation, position, and size and to obtain the distribution of the set of structures, or shapes in the morphospace, General Procrustes Analysis and superimposition were applied (Dryden and Mardia, 1998; Rohlf and Slice, 1990, Klingenberg, 2011). To test the effect of allometry and eliminate the size-related changes in the morphological traits, a multivariate regression of the Procrustes coordinates (structure shape) to the centroid size (structure size) was performed. Phenotypic variations were analyzed and visualized using Principal Component Analysis (PCA) and Canonical Variate Analysis (CVA) on the Procrustes coordinates, or regression residuals in the case of statistically significant results for

allometry (Klingenberg, 2011). PCA and CVA graphs were used to visualize the distribution of individuals within the treatments (based on the morphology of the structures examined) in the morphospace defined by the PC and CV axes, with confidence ellipses calculated as the mean values for each treatment, i.e., group (Klingenberg, 2011). Specific changes in the shape and size of the structures were visualized using wireframe and outline graphs obtained by MorphoJ software.

3 RESULTS

3.1 Results of the deformity rate analysis

Visual analysis of the morphological structures revealed a total of 15 mandibles, 14 mentums and zero wings with some form of malformation or damage.

Among the mandibles (out of a total of 275 mandibles photographed for the entire experiment), only 10 (3.64 % of the total sample) were visibly deformed (four in the 2.5 NP treatment, one in the 25 NP treatment, two in the 2500 NP treatment and three in the control, in the form of the lack of an apical tooth, complete curvature of the mandible or an additional internal tooth), and 5 were completely worn out (Supplementary Figure 1).

Among the mentums (out of the total of 275 mentums photographed for the entire experiment), only 4 (1.45 %) were visibly deformed (two in the 2.5 NP treatment with deformations of the central tooth, one in the 25 NP treatment - additional tooth on the central tooth, and one in the control - the gap between the central and lateral teeth) and 10 were visibly broken or undeveloped (Supplementary Figure 2).

The percentage of deformed and worn-out structures was extremely low in relation to the total sample, so it was not possible to statistically analyze the results and determine the deformity rate.

3.2. Results of the geometric morphometric analysis

Morphological structures with some form of malformation or damage, detected by the visual analysis described in the previous subsection 3.1 (a total of 15 mandibles and 14 mentums), were excluded from further geometric morphometric analysis. Additionally, 2 mandibles (0.8 % of the total sample), 29 mentums (11.1 % of the total sample), and 0 male and 5 female wings (6.6 % of the total sample) with "extreme" values of the morphological parameters were observed using the MorphoJ software, which were also excluded from further analysis (Table 1).

3.2.2 Mandibles

Significant differences in mandible size were revealed (ANOVA, $F = 134.7$; $p < 0.001$), with the following groups significantly differing in centroid size (*post hoc* Tukey test $p < 0.05$): the control from all other treatments, and the 2500 NP treatment from all other treatments. Significant differences were also revealed in the mandible shape (MANOVA, Willks'$\lambda = 0.23$; $F = 3$; $p < 0.001$), therefore further geometric morphometric analysis was conducted.

Regression analysis showed that a total of 3.05 % of changes in shape were caused by differences in size and that this percentage of allometry, although very small, was statistically significant ($p < 0.005$), therefore further analysis was performed on regression residuals.

PCA analysis (Supplementary Table 1) showed the tendency of grouping for mandibles treated with the highest concentration of 2500 mg kg^{-1} CeO_2. Along the PC2 axis (describing 13.47 % of the total variability), the control and groups treated with lower CeO_2 NP concentrations overlapped in the positive part, while the group treated with the highest concentration of 2500 CeO_2 NP stood out in the negative part of the axis and was characterized by widening of the base, retreating of the first and second inner teeth towards the base, and elongation of the apical tooth (Figure 2a).

CVA analysis (Supplementary Table 2) revealed clearer separation of the groups, with visible overlapping between some treatments (Figure 2b). Along the CV1 axis (explaining 55.28 % of the total variability) the grouping of the control, 25 and 250 NP treatments in the negative part, and separation from the 2.5 and 2500 NPs treatments in the positive part of the axis was observed. The CV2 axis (27.64 % of the total variability) showed slight separation of the control and the group treated with the lowest concentration from the other groups. Visualization using "Outline" and "Transformation grid" graphics confirmed the trend observed by PCA analysis – in the treated individuals, the base of the mandible expanded, with shortening of the mandibular joint, compaction of internal teeth and elongation of the apical tooth. The analysis revealed the greatest changes in the apical tooth (LM 1 and 2) and the tendency for it to elongate with increasing CeO_2 NP concentrations. Visible changes were observed in the first and second internal teeth, i.e., LMs 4, 6 and 8 which described the bases of the teeth. Separation of the groups was confirmed by the values of Mahalanobis distances, showing significant differences between all groups, except between the control and 25 and 250 NP treatments (Supplementary Table 3).

3.2.3 Mentums

Significant differences in the mentum size were revealed (ANOVA, $F = 3.92$; $p = 0.004$), with the 250 NP treatment (larger CS) significantly differing from the 2.5 and 25 NP treatments (smaller CS) (*post hoc* Tukey test $p < 0.05$). Significant differences were also revealed in the mentum shape (MANOVA, Willks'$\lambda = 0.3354$; $F = 2$; $p < 0.001$), therefore further geometric morphometric analysis was conducted.

Regression analysis showed that a total of 3.93 % of changes in shape were caused by differences in size and that this percentage of allometry, although very small, was statistically significant ($p < 0.005$), therefore further analysis was performed on the regression residuals.

PCA analysis (Supplementary Table 4) indicated the grouping of the control and groups treated with lower concentrations (2.5; 25 and 250 NPs treatments) in the positive part of the PC2 axis (which carries 22.64 % of the total variability), which were characterized by shorter teeth with wider bases. In the negative part of the axis, the group treated with the highest concentration (2500 NP treatment) stood out, characterized by mentums with elongated teeth and a narrowed base of the central trifid tooth (Figure 3a).

CVA analysis (Supplementary Table 5) revealed visible overlapping between some treatments, with visible separation of the 2500 NP treatment (Figure 3b). Along the CV1 axis (explaining 53.74 % of the total variability), the group treated with the highest concentration of 2500 mg kg^{-1} CeO_2 NPs was clearly separated in the positive part from the control and other groups, which were located in the negative part of the axis. According to the CV2 axis (20.47 %), group separation was weaker, but a gradual distribution of groups, from the control, through the lower to higher concentrations, was observed. Associated graphs revealed that with increasing

NP concentrations there was a very weak expansion of the mentum base (with a large variation of LMs 1 and 29) and an expansion of the base of two internal lateral teeth, however at high concentrations there was a large elongation of all teeth, with prominent retraction of the central tooth base (LMs 12, 14, 16 and 18), and inner lateral tooth elongation (LMs 11 and 19). Mahalanobis distances confirmed significant differences between all groups, except between the 25 and 250 NP treatments (Supplementary Table 6).

3.2.4 Wings

Significant differences in wing size between the sexes were revealed (ANOVA, $F = 8.74$, $P = 0.003$), with control females having significantly larger CS from the control males (*post hoc* Tukey test $p < 0.05$). The following treated groups showed significant differences in centroid size (*post hoc* Tukey test $p < 0.05$): the control group of females (larger CS) differed from males in the 2500 and 250 NP treatments (smaller CS); males in the 2500 NP treatment (smaller centroid size) differed from females in the 25 and 250 NP treatments (larger centroid size). Significant differences between the sexes were also revealed in wing shape (MANOVA, Willks'$\lambda = 0.003$; $F = 4.925$; $p < 0.001$).

PCA analysis (Supplementary Figure 1) showed the separation of females and males along the PC1 axis (64.12 % of the total variability). Analysis revealed that in females, LMs 4 to 11 moved toward the circumference of the wing, i.e., widened, whilst LMs 1, 2 and 3 moved toward the inside of the wing. In males the situation was reversed, with most prominent changes noticeable in LMs 12 and 13.

Regression analysis showed that a total of 5.54 % of changes in shape were caused by differences in size and that this percentage of allometry, although very small, was statistically

significant ($p < 0.005$). The regression analysis graph shows that the size varied considerably in the total sample in both sexes, females having larger wings than males, but with size differences slightly diminishing with the CeO_2 NP treatment (Supplementary Figure 2).

Due to the existence of sexual dimorphism, i.e., statistically significant differences between males and females in wing size and shape, further analyses were performed for each sex independently.

Female wings

Significant differences in female wing size were revealed (ANOVA, $F = 4.01$; $p = 0.006$), with the control treatment (larger CS) significantly differing from the 2.5 and 2500 NP treatments (smaller CS) (*post hoc* Tukey test $p < 0.05$). Significant differences were also revealed in the female wing shape (MANOVA, Willks'$\lambda = 0.0564$; $F = 2.19$; $p < 0.01$), therefore further geometric morphometric analysis was conducted.

Regression analysis showed that a total of 2.86 % of changes in shape were caused by differences in size and that this percentage of allometry was not statistically significant ($p > 0.05$), therefore further analysis was performed on Procrustes coordinates.

PCA analysis (Supplementary Table 7) showed extensive differentiation between the groups, however, individuals from the treated groups were mostly in the positive part of the PC1 axis (31.60 % variability) and were characterized by elongated wing bases with elongated anal nerves and radio-medial nerves shifted to the wing base; in contrast, the individuals from the control group were located mainly in the negative part of the axis and had the opposite characteristics (Figure 4a).

CVA analysis (Supplementary Table 8) revealed the clear separation and grouping of several treatments (Figure 4b). The 25 and 250 NP treatments were grouped together in the positive part of the CV1 axis (62.03 % of the total variability) and were characterized by a slight narrowing of the wing base with a slight elongation of the distal wing circumference and elongation of the anal nerve and subcostal nerve (LMs 4, 6 and 9). However, according to the second CV axis (describing 17.67 % of the variability), the groups treated with the lowest and highest concentrations, 2.5 and 2500 mg kg^{-1} CeO_2 NPs were grouped together in its positive part and were characterized by elongation of the wing base (LMs 1, 2 and 3) and retraction of the radio-medial nerve to the base (LMs 12 and 13), elongation of the anal nerve (LM 4), reduction of the distance between the tips of the cubital and medial nerve (LMs 5, 6 and 7) and retraction the subcostal and first radial nerve tips towards the base of the wing (LMs 9 and 10). The control group stood out from the others in the negative part of both axes. Mahalanobis distances showed a statistically significant difference between all groups except between the 25 and 250 NP treatments (Supplementary Table 9).

Male wings

Significant differences in the male wing size were revealed (ANOVA, $F = 4.47$; $p = 0.003$), with 2.5 and 25 NP treatments (larger CS) significantly differing from the 2500 NP treatment (smaller CS) (*post hoc* Tukey test $p < 0.05$). Significant differences were also revealed in the male wing shape (MANOVA, Willks'$\lambda = 0.055$; $F = 1.872$; $p < 0.001$), therefore further geometric morphometric analysis was conducted.

Regression analysis showed that a total of 2.348 % of the changes in shape were caused by differences in size and that this percentage of allometry was not statistically significant ($p > 0.05$), therefore further analysis was performed on Procrustes coordinates.

PCA analysis (Supplementary Table 6) showed large overlaps between the groups, with just individuals from the 250 NP treatment slightly separating from others (Supplementary Figure 3).

CVA analysis (Supplementary Table 10) revealed clearer separation of the groups, but still with visible overlapping between some treatments (Figure 5). Based on the CV1 axis (47.84 % of the total variability), a large group overlap was observed, with the group treated with the highest concentration, 2500 mg kg^{-1} CeO_2, positioned in the center, and the control group predominantly in the negative part (wider wings in the middle part, LMs 4, 5, 10 and 11). Based on the CV3 axis (16.71 % of the total variability), the group treated with the highest concentration stood out from the other groups in the negative part and was characterized by dilation of the wing base (LMs 1, 2 and 3), elongation of the anal nerve (LMs 3 and 4), median nerve elongation (LM 6) and subcostal nerve shortening (LM 10). No specific pattern of wing shape variation with respect to the amount of nanoparticles could be observed. Mahalanobis distances showed a statistically significant difference between all groups (Supplementary Table 11).

4 DISCUSSION

In the last two decades, a large amount of data has emerged on the potential effects of engineered nanomaterial on benthic freshwater biota. It is suggested that effects at the level of organisms, species and entire communities (e.g., impact on growth and reproduction) can

further be expected in the future if the expansion of nanotechnology continues (Mahaye et al., 2017).

In general, CeO_2 NPs are known for their positive biological effects, which is why they have found application in medicine (Zhang et al., 2017; 2011), however, many studies have shown CeO_2 NP toxic effects when *Daphnia* (García et al., 2011; Lee et al. 2009), chironomids (Savić-Zdravković et al., 2020; Lee et al., 2009), mollusks (Koehle-Divo et al., 2018), nematodes (Roh et al., 2010; Zhang et al., 2011) and algae (Manier et al., 2011; Rogers et al., 2010) are exposed to them, highlighting that, regardless of their usefulness, CeO_2 NPs can have a negative impact on the environment.

The standard recommended parameters for assessing the impact of stressors on chironomids in the latest literature are mortality, immobilization (impact on movement), eclosion (from pupae to adult stage), and growth (OECD, 2004). These parameters are commonly used in applied and scientific studies, but great efforts are being made to determine new, sub lethal responses to stressors, such as behavioral changes (De Bisthoven et al., 2004), changes in gene expression (Park and Choi, 2017), biochemical and metabolic effects (Long et al., 2015) and morphological changes (Tomilina et al., 2020; 2015). The reason for this is the need to develop meaningful bioassays which can provide reliable information on the impact of contaminants (especially at environmentally relevant concentrations), meaningful indication of stress, and which are specific enough to distinguish the effects of different contaminants (Hines et al., 2010; Jeppe et al., 2014). Chironomid deformities have been used as sensitive indicators of stress in many studies assessing the impact of human activities on aquatic ecosystems (Arambourou 2019; 2012; Tomilina et al., 2020; 2015). The exact cause and mechanisms of deformities have

not been precisely determined, and they are considered to be regulated by a large number of factors (Gagliardi, 2017). However, it is assumed that deformations during macroinvertebrate ontogeny may occur due to: disturbances in endocrine regulation during molting (Salmelin et al., 2015; Meregalli and Ollivier, 2001); gene expression disorders (Planello et al., 2015); or increased protein synthesis caused by an increase in the number of active nucleoli in polytene chromosomes (which leads to increased resistance to toxins, but causes deformities) (Meregalli et al., 2002), which may have a potential genotoxic, carcinogenic and mutagenic effect manifested in the phenotype.

In the present study, visible damage and malformations were observed in chironomid larval mouthparts (mentums and mandibles), however, this was an extremely small percentage in relation to the total sample. The changes were mainly the lack of an apical tooth or the complete elongation of the entire mandibular structure, as well as the loss of or an extra tooth in the mentums. The influence of CeO_2 NPs on the occurrence of deformities in chironomids has, to our knowledge, so far been examined only in the study by Bour et al. (2015), in which no significant teratogenic effect of CeO_2 NPs was observed. Many studies question the reliability of the use of visible chironomid deformations as a biomarker, primarily due to the high rate of deformities observed in natural populations (Langer-Jaesrich et al., 2010), and even in laboratory populations (7 % to 34 %), both in the controls and specimens exposed to different stressors (de Bisthoven et al., 2001; 1998; Meregalli and Ollevier, 2001; Meregalli et al., 2001). Similarly, in the present study, deformed individuals were observed in both the controls and treatments, however, deformity rates were lower than those recorded in the literature (1.45 % in the mentums and 3.64 % in the mandibles). Furthermore, it cannot be stated with certainty whether

the malformations in the structures were really deformities, or whether they were damage caused by the substrate, or even during the preparation of the microscope slides. Morphological analyses, in many disciplines, have long since moved from descriptive (description of the appearance of deformities) to quantitative methods of analysis (Bookstein, 1998). For these reasons, a further assessment of the influence of CeO_2 NPs on the morphological variability of chironomids through a precise and reproducible method of geometric morphometry was conducted. The greatest influence was shown on the morphological structures of the larvae, but also on the structures of adult individuals. Already in PCA analysis, the larvae treated with the highest CeO_2 NP concentrations (2500 mg kg^{-1}) stood out from all the other treatments by the shape and size of the mouthparts (mandibles and mentum); in CVA analysis the separation was even clearer. The mandibles of treated individuals were characterized by the expansion of the base, with the shortening of the first and second internal teeth towards the base, and the largest changes were observed on the apical tooth, which tends to elongate at high CeO_2 NP concentrations. A significant difference in the mandible shape was found between all groups, except between the control and the group treated with 25 and 250 CeO_2 NPs, indicating a similar morphological variability of individuals exposed to these two concentrations. The most prominent changes in mentum shape occurred at low (2.5 mg kg^{-1}) and very high CeO_2 NP concentrations (2500 mg kg^{-1}). With increasing concentration of CeO_2 NPs there was a slight expansion of the base and the two internal lateral teeth; however, with extremely high concentrations, there was a sudden elongation of all teeth, with a great retraction of the base of the central tooth, and elongation of the tips of internal lateral teeth. As evident above, our analyses have shown significant teratogenic effects on the morphological structures that are

considered to be extremely uniform and unchanging and are most often used in chironomid identification (Vallenduuk, 2017; Armitage et al., 2012). Although the characteristics of the external anatomy of chironomids are extremely conservative structures, our results prove that they show sensitivity to the presence of CeO_2 NPs, revealing the potential for triggering further consequences (i.e., changes in metabolism, diet or behavior).

The method of geometric morphometry has been used primarily to address the issue of species differences and analyze sexual dimorphism (Lorenz et al., 2017). In the present analysis of chironomid adults, the existence of full dimorphism was confirmed in the size and shape of the wings in *C. riparius* by the method of geometric morphometry, which is the first analysis of this type of chironomids in the literature so far. Analysis revealed that females have wider wings with a shortened proximal section, whereas in males the situation is reversed, i.e., the wings are narrower, primarily in the central part, with an elongated proximal section, i.e., the base of the wing, with a displaced radio-medial nerve towards the distal part of the wing. Further analysis showed the effect of treatment on the shape and size of the wings of both sexes. PCA analysis of female wings showed that the treated individuals were characterized by elongated wing bases with an elongated anal and radio-medial nerve shifted to the wing base, while CVA analysis showed the greatest changes in individuals treated with the lowest and highest concentrations (2.5 and 2500 mg kg^{-1} CeO_2 NPs): elongation of the wing base, retraction of the radio-medial nerve towards the base, elongation of the anal nerve, reduction of the distance between the tips of the cubital and medial nerve, and pulling of the tips of the subcostal and first radial nerve towards the base of the wing. These female individuals also had smaller wings than average, which may explain the reduction in gender differences observed by regression analysis. There is

a significant difference between all groups, except between the 25 and 250 CeO_2 NP treatments, as in the case of the mentum. Male wings showed less response to nanoparticle treatment, and although there was a significant difference between all groups, no specific pattern of variation in wing shape relative to the amount of nanoparticles could be observed. The group treated with the highest concentration stood out from all the others only according to the CV3 axis, and it was characterized by the expansion of the wing base, elongation of the anal nerve, elongation of the medial nerve and shortening of the subcostal nerve. More pronounced morphological variability in females responding to environmental stress has previously been registered within dipterans in the study by Cvetković et al. (2020), which should be the focus of further ecotoxicological studies. The existence of a large number of unanswered questions in the analysis of the occurrence of deformities in chironomids indicates the need to develop more precise and comprehensive methods in future studies.

The pattern of CeO_2 NP effects on adult chironomids might be twofold: NPs induce effects at the larval stage, causing the developmental disorder of adult individuals; or adult individuals retain NPs in their bodies that affect them at this stage of development, which can lead to the potential inter-ecosystem transfer of nanoparticles. Differences in the aggregation levels of CeO_2 NPs, associated with different concentrations, could have contributed to the difference in the larval uptake. Previously, we showed that the increase in the uptake of CeO_2 NPs by chironomid larvae is not linear with increasing concentrations (Savić-Zdravković et al., 2020). This may explain why in some of the observed results there is not a clear dose-response effect, since lower concentrations may show more effect. Bundschuh et al. (2019) examined the inter-ecosystem transfer of NPs via the food chain in flowing microcosms for the first time. It has

been confirmed that Trichoptera (*Chaetopteryx villosa*) transmit nano-TiO_2 and nano-gold to their terrestrial stages, and these NPs have been shown to delay flight and reduce energy reserves (measured over the total amount of lipids) in adults. According to the most pessimistic estimates, it is assumed that terrestrial predators (e.g., bats) that feed on aquatic insects can ingest up to three times more NPs than usual, and such prey may have lower nutritional value, which can lead to negative consequences at the meta-ecosystem level (Bundschuh et al., 2019). In the same study, Bundschuh et al. (2019) indicated that NPs that reach aquatic from terrestrial media can be returned to the terrestrial environment via macroinvertebrates that have terrestrial adult stages. There is a chance that chironomids transfer NPs from the larval to adult stages in a similar way, and if their enormous biomass is considered (Armitage et al., 2012), much larger consequences can be expected. Recent studies have predicted that CeO_2 NP concentrations may be higher than currently thought and that the annual inflow of CeO_2 NPs is 0.1 to 10 μg l^{-1} in surface water, or even between 10 and 100 mg kg^{-1} in landfills, through which nanoparticles can reach freshwater ecosystems and increase current concentrations in sediments (Wang and Novichak, 2018). Point sources of wastewater discharge and accumulation can further potentially increase the CeO_2 NP concentration. If we add to this the fact that our previous research confirmed the bioaccumulation of CeO_2 NPs in chironomids, there is a real risk of the trophic transfer of NPs, with consequences for other aquatic and terrestrial organisms. Taking into account both previous studies and the research results within this paper, it is necessary to emphasize the evident need to standardize the ecotoxicological testing of nanoparticles, which could ensure the uniformity, precision and accuracy of future ecotoxicological tests. Improving the testing methodology can greatly improve the further

monitoring of the state of aquatic ecosystems and the biomonitoring of pollution by nanoparticles, and thus the possibility of early purification and remediation.

4.1. Conclusions

In conclusion, small, but still significant, changes in important morphological structures of larvae and adults were observed at low and very high concentrations of CeO_2 NPs, as well as the potential impact on reducing sexual dimorphism. These results indicate that the sublethal changes observed in chironomids due to exposure to CeO_2 nanoparticles are significant and may potentially lead to further changes, which may lead to repercussions of as yet unexamined proportions. With respect to the potential of chironomids to bioaccumulate nanoparticles, and the observed influence at both larval and adult stages, there is a real risk of trophic transfer of NPs, with consequences for other organisms in the aquatic and terrestrial food chain.

A geometric morphometric approach proved to be an exceptional tool in assessing the teratogenic effects of CeO_2 NPs, considering that the effects could be easily qualified and quantified, and the exact morphological changes visualized using MorphpoJ software (Klingenberg, 2011). With regard to the other advantages of the geometric morphometric method (precision, uniformity, the possibility of accurate visualization of fine changes using computer software), and the latest recommendations of the scientific community, it shows great potential for application in ecotoxicology, and can significantly supplement the existing ecotoxicological testing of nanoparticles.

Acknowledgment—The authors would like to express their gratitude to Nikola Stanković and Jelena Stanković, from Faculty of Science and Mathematics, University of Niš, as well as Janja Vidmar, from Jožef Stefan Institute in Slovenia, for their invaluable expertise help provided during experimental phase of our research.

Funding- This work was supported by the Ministry of Education, Science, and Technological Development, Republic of Serbia (grant III43002).

REFERENCES

Al-Shami, S.A., Salmah, M.R.C., Hassan, A.A. and Azizah, M.N.S., 2011. Evaluation of mentum deformities of Chironomus spp. (Chironomidae: Diptera) larvae using modified toxic score index (MTSI) to assess the environmental stress in Juru River Basin, Penang, Malaysia. Environmental monitoring and assessment, 177(1-4), pp.233-244. URL: https://link.springer.com/article/10.1007/s10661-010-1630-1

Anderson, P.D. and D'Apollonia, S., 1978. Aquatic animals. Principles of Ecotoxicology. John Wiley & Sons, New York, pp.187-221. URL: https://pdfs.semanticscholar.org/f5d3/51218448fcb7816fe32837bef0c4ec32e431.pdf

Arambourou, H., Planelló, R., Llorente, L., Fuertes, I., Barata, C., Delorme, N., Noury, P., Herrero, Ó., Villeneuve, A. and Bonnineau, C., 2019. *Chironomus riparius* exposure to field-collected contaminated sediments: from subcellular effect to whole-organism response. Science of The Total Environment, 671, pp.874-882. DOI: https://doi.org/10.1016/j.scitotenv.2019.03.384

Arambourou, H., Beisel, J.N., Branchu, P. and Debat, V., 2012. Patterns of fluctuating asymmetry and shape variation in *Chironomus riparius* (Diptera, Chironomidae) exposed to nonylphenol or lead. PloS one, 7(11). DOI: https://doi.org/10.1371/journal.pone.0048844

Armitage, P.D., Pinder, L.C. and Cranston, P.S. eds., 2012. The Chironomidae: biology and ecology of non-biting midges. Springer Science & Business Media. URL: https://books.google.rs/books?id=DHPyCAAAQBAJ&lpg=PR10&ots=QU2QL6skRG&dq=Armitage%20Cranston%201995%20The%20chironomidae&lr&pg=PR10#v=onepage&q=Armitage%20Cranston%201995%20The%20chironomidae&f=false

Artells, E., Issartel, J., Auffan, M., Borschneck, D., Thill, A., Tella, M., Brousset, L., Rose, J., Bottero, J.Y. and Thiery, A., 2013. Exposure to cerium dioxide nanoparticles differently affect swimming performance and survival in two daphnid species. PloS one, 8(8). DOI: https://doi.org/10.1371/journal.pone.0071260

Batac-Catalan, Z. and White, D.S., 1982. Creating and maintaining cultures of *Chironomus tentans* (Diptera: Chironomidae). Entomological News, 93, pp.54-58. URL: https://biostor.org/pdfproxy.php?url=https%3A%2F%2Farchive.org%2Fdownload%2Fbiostor-77149%2Fbiostor-77149.pdf

Bayat, N., Lopes, V.R., Schoelermann, J., Jensen, L.D. and Cristobal, S., 2015. Vascular toxicity of ultra-small TiO2 nanoparticles and single walled carbon nanotubes in vitro and in vivo. Biomaterials, 63, pp.1-13. DOI: https://doi.org/10.1016/j.biomaterials.2015.05.044

Bookstein, F.L., 1998. A hundred years of morphometrics. Acta Zoologica Academiae

Bour, A., Mouchet, F., Verneuil, L., Evariste, L., Silvestre, J., Pinelli, E. and Gauthier, L., 2015a. Toxicity of CeO_2 nanoparticles at different trophic levels–effects on diatoms, chironomids and amphibians. Chemosphere, 120, pp.230-236. DOI: https://doi.org/10.1016/j.chemosphere.2014.07.012

Boxall, A.B., Chaudhry, Q., Ardern-Jones, A., Jefferson, B., Watts, C.D., Sinclair, C., Baxter-Jones, A.D., Aitken, R., Watts, C. and Chaudrhry, Q., 2008. Current and future predicted environmental exposure to engineered nanoparticles. Report by the Central Science Laboratory (CSL) York for the Department of the Environment and Rural Affairs (DEFRA), UK. URL: http://www.defra.gov.uk/science/Project_Data/DocumentLibrary/CB01098/CB01098_6270_FRP.pdf

Bundschuh, M., Englert, D., Rosenfeldt, R.R., Bundschuh, R., Feckler, A., Lüderwald, S., Seitz, F., Zubrod, J.P. and Schulz, R., 2019. Nanoparticles transported from aquatic to terrestrial ecosystems via emerging aquatic insects compromise subsidy quality. Scientific reports, 9(1), pp.1-8. URL: https://www.nature.com/articles/s41598-019-52096-7

Bundschuh, M., Filser, J., Lüderwald, S., McKee, M.S., Metreveli, G., Schaumann, G.E., Schulz, R. and Wagner, S., 2018. Nanoparticles in the environment: where do we come from, where do we go to?. Environmental Sciences Europe, 30(1), pp.1-17. URL: https://enveurope.springeropen.com/articles/10.1186/s12302-018-0132-6

Collin, B., Auffan, M., Johnson, A.C., Kaur, I., Keller, A.A., Lazareva, A., Lead, J.R., Ma, X., Merrifield, R.C., Svendsen, C. and White, J.C., 2014. Environmental release, fate and ecotoxicological effects of manufactured ceria nanomaterials. Environmental Science: Nano, 1(6), pp.533-548. URL: https://pubs.rsc.org/en/content/articlelanding/2014/EN/C4EN00149D#!divAbstract

Cvetković, V. J., Jovanović, B., Lazarević, M., Jovanović, N., Savić-Zdravković, D., Mitrović, T., & Žikić, V. (2020). Changes in the wing shape and size in *Drosophila melanogaster* treated with food grade titanium dioxide nanoparticles (E171)–A multigenerational study. Chemosphere, 261, 127787. DOI: https://doi.org/10.1016/j.chemosphere.2020.127787

De Bisthoven, L.J., Gerhardt, A. and Soares, A.M., 2004. Effects of acid mine drainage on larval *Chironomus* (Diptera, Chironomidae) measured with the multispecies freshwater Biomonitor®. Environmental Toxicology and Chemistry: An International Journal, 23(5), pp.1123-1128. DOI: https://doi.org/10.1897/02-603

De Bisthoven, L.J., Postma, J., Vermeulen, A., Goemans, G. and Ollevier, F., 2001. Morphological deformities in *Chironomus riparius* Meigen larvae after exposure to cadmium over several generations. Water, Air, and Soil Pollution, 129(1-4), pp.167-179. URL: https://link.springer.com/article/10.1023/A:1010367524314

De Bisthoven, L.J., Postma, J.F., Parren, P., Timmermans, K.R. and Ollevier, F., 1998. Relations between heavy metals in aquatic sediments and in Chironomus larvae of Belgian lowland rivers and their morphological deformities. Canadian Journal of Fisheries and Aquatic Sciences, 55(3), pp.688-703. DOI: https://doi.org/10.1139/f97-265

Di Veroli, A., Santoro, F., Pallottini, M., Selvaggi, R., Scardazza, F., Cappelletti, D. and Goretti, E., 2014. Deformities of chironomid larvae and heavy metal pollution: from laboratory to field studies. Chemosphere, 112, pp.9-17. DOI: https://doi.org/10.1016/j.chemosphere.2014.03.053

Gagliardi, B.S., 2017. *Differentiating pollutant-induced effects from non-contaminant stress responses in aquatic midges (Diptera: Chironomidae) (Doctoral dissertation).* URL: https://minerva-access.unimelb.edu.au/handle/11343/193008

Garaud, M., Trapp, J., Devin, S., Cossu-Leguille, C., Pain-Devin, S., Felten, V. and Giamberini, L., 2015. Multibiomarker assessment of cerium dioxide nanoparticle ($nCeO_2$) sublethal effects on two freshwater invertebrates, *Dreissena polymorpha* and *Gammarus roeseli*. Aquatic Toxicology, 158, pp.63-74. DOI: https://doi.org/10.1016/j.aquatox.2014.11.004

García, A., Espinosa, R., Delgado, L., Casals, E., González, E., Puntes, V., Barata, C., Font, X. and Sánchez, A., 2011. Acute toxicity of cerium oxide, titanium oxide and iron oxide nanoparticles using standardized tests. Desalination, 269(1-3), pp.136-141. DOI: https://doi.org/10.1016/j.desal.2010.10.052

Gottschalk, F., Lassen, C., Kjoelholt, J., Christensen, F. and Nowack, B., 2015. Modeling flows and concentrations of nine engineered nanomaterials in the Danish environment. International journal of environmental research and public health, 12(5), pp.5581-5602. DOI: https://doi.org/10.3390/ijerph120505581

Giese, B., Klaessig, F., Park, B., Kaegi, R., Steinfeldt, M., Wigger, H., von Gleich., A., & Gottschalk, F. (2018). Risks, release and concentrations of engineered nanomaterial in the environment. Scientific reports, 8(1), 1-18. https://doi.org/s41598-018-19275-4

Hamilton, A.L. and Saether, O.A., 1971. The occurrence of characteristic deformities in the chironomid larvae of several Canadian lakes. The Canadian Entomologist, 103(3), pp.363-368. DOI: https://doi.org/10.4039/Ent103363-3

Hines, A., Staff, F.J., Widdows, J., Compton, R.M., Falciani, F. and Viant, M.R., 2010. Discovery of metabolic signatures for predicting whole organism toxicology. Toxicological Sciences, 115(2), pp.369-378. DOI: https://doi.org/10.1093/toxsci/kfq004

Hund-Rinke, K., Baun, A., Cupi, D., Fernandes, T.F., Handy, R., Kinross, J.H., Navas, J.M., Peijnenburg, W., Schlich, K., Shaw, B.J. and Scott-Fordsmand, J.J., 2016. Regulatory ecotoxicity testing of nanomaterials–proposed modifications of OECD test guidelines based on laboratory experience with silver and titanium dioxide nanoparticles. Nanotoxicology, 10(10), pp.1442-1447. DOI: https://doi.org/10.1080/17435390.2016.1229517

Hoffmann, A.A., Woods, R.E., Collins, E., Wallin, K., White, A., McKenzie, J.A., 2005. Wing shape versus asymmetry as an indicator of changing environmental conditions in insects. Aust. J. Entomol. 44 (3), 233e243.

Hornyak, G.L., Moore, J.J., Tibbals, H.F. and Dutta, J., 2018. Fundamentals of nanotechnology. CRC press. URL:

https://books.google.rs/books?id=mf7KBQAAQBAJ&lpg=PP1&ots=hTzbRXtv_i&dq=Hornyak%20NANOTECHNOLOGY&lr&pg=PA5#v=onepage&q=Hornyak%20NANOTECHNOLOGY&f=false

Ivanović, A., Kalezić, M. 2009. "Evoluciona morfologija - teorijske postavke i geometrijska morfometrija", Biološki fakultet Beograd, Str 216, ISBN: 978-86-7078-055-2, COBISS. SR-ID 157935116

Jeppe, K.J., Carew, M.E., Long, S.M., Lee, S.F., Pettigrove, V. and Hoffmann, A.A., 2014. Genes involved in cysteine metabolism of *Chironomus tepperi* are regulated differently by copper and by cadmium. Comparative Biochemistry and Physiology Part C: Toxicology & Pharmacology, 162, pp.1-6. DOI: https://doi.org/10.1016/j.cbpc.2014.02.006

Kendall, D.G., 1977. The diffusion of shape. Advances in applied probability, 9(3), pp.428-430. DOI: https://doi.org/10.2307/1426091

Klingenberg, C. P., 2011. MorphoJ: an integrated software package for geometric morphometrics. Molecular Ecology Resources 11: 353-357. DOI: https://doi.org/10.1111/j.1755-0998.2010.02924.x

Koehle-Divo, V., Cossu-Leguille, C., Pain-Devin, S., Simonin, C., Bertrand, C., Sohm, B., Mouneyrac, C., Devin, S. and Giambérini, L., 2018. Genotoxicity and physiological effects of CeO_2 NPs on a freshwater bivalve (*Corbicula fluminea*). Aquatic Toxicology, 198, pp.141-148. DOI: https://doi.org/10.1016/j.aquatox.2018.02.020

Langer-Jaesrich, M., Köhler, H.R. and Gerhardt, A., 2010. Can mouth part deformities of *Chironomus riparius* serve as indicators for water and sediment pollution? A laboratory approach. Journal of soils and sediments, 10(3), pp.414-422. URL: https://link.springer.com/article/10.1007/s11368-010-0195-5

Lead, J.R., Batley, G.E., Alvarez, P.J., Croteau, M.N., Handy, R.D., McLaughlin, M.J., Judy, J.D. and Schirmer, K., 2018. Nanomaterials in the environment: behavior, fate, bioavailability, and effects—an updated review. Environmental toxicology and chemistry, 37(8), pp.2029-2063. DOI: https://doi.org/10.1002/etc.4147

Lee, S.W., Kim, S.M. and Choi, J., 2009. Genotoxicity and ecotoxicity assays using the freshwater crustacean *Daphnia magna* and the larva of the aquatic midge *Chironomus riparius* to screen the ecological risks of nanoparticle exposure. Environmental toxicology and pharmacology, 28(1), pp.86-91. DOI: https://doi.org/10.1016/j.etap.2009.03.001

Long, S.M., Tull, D.L., Jeppe, K.J., De Souza, D.P., Dayalan, S., Pettigrove, V.J., McConville, M.J. and Hoffmann, A.A., 2015. A multi-platform metabolomics approach demonstrates changes in energy metabolism and the transsulfuration pathway in *Chironomus tepperi* following exposure to zinc. Aquatic toxicology, 162, pp.54-65. DOI: https://doi.org/10.1016/j.aquatox.2015.03.009

Lorenz, C., Almeida, F., Almeida-Lopes, F., Louise, C., Pereira, S.N., Petersen, V., Vidal, P.O., Virginio, F. and Suesdek, L., 2017. Geometric morphometrics in mosquitoes: What has been measured?. Infection, Genetics and Evolution, 54, pp.205-215. DOI: https://doi.org/10.1016/j.meegid.2017.06.029

Manier, N., Garaud, M., Delalain, P., Aguerre-Chariol, O. and Pandard, P., 2011. Behaviour of ceria nanoparticles in standardized test media–influence on the results of ecotoxicological tests. In Journal of Physics: Conference Series (Vol. 304, No. 1, p. 012058). IOP Publishing. URL: https://iopscience.iop.org/article/10.1088/1742-6596/304/1/012058/pdf

Mahaye, N., Thwala, M., Cowan, D.A. and Musee, N., 2017. Genotoxicity of metal based engineered nanoparticles in aquatic organisms: A review. Mutation Research/Reviews in Mutation Research, 773, pp.134-160. DOI: https://doi.org/10.1016/j.mrrev.2017.05.004

Markert, B.A., Breure, A.M. and Zechmeister, H.G. eds., 2003. Bioindicators and biomonitors. Elsevier. URL: https://www.sciencedirect.com/bookseries/trace-metals-and-other-contaminants-in-the-environment/vol/6?page-size=100&page=1

Martinez, E.A., Moore, B.C., Schaumloffel, J. and Dasgupta, N., 2002. The potential association between menta deformities and trace elements in Chironomidae (Diptera) taken from a heavy metal contaminated river. Archives of Environmental Contamination and Toxicology, 42(3), pp.286-291. URL: https://link.springer.com/article/10.1007/s00244-001-0190-0

Meregalli, G., Bettinetti, R., Pluymers, L., Vermeulen, A.C., Rossaro, B. and Ollevier, F., 2002. Mouthpart deformities and nucleolus activity in field-collected *Chironomus riparius* larvae. Archives of environmental contamination and toxicology, 42(4), pp.405-409. DOI: https://doi.org/10.1007/s00244-001-0040-3

Meregalli, G. and Ollevier, F., 2001. Exposure of *Chironomus riparius* larvae to 17α-ethynylestradiol: effects on survival and mouthpart deformities. Science of the total environment, 269(1-3), pp.157-161. DOI: https://doi.org/10.1016/S0048-9697(00)00824-X

OECD, Organisation for Economic Co-operation and Development, 2020: OECD Guidelines for the Testing of Chemicals, Section 2. Effects on Biotic Systems. https://doi.org/10.1787/20745761

OECD, Organisation for Economic Co-operation and Development, 2019: GUIDANCE DOCUMENT ON AQUEOUS-PHASE AQUATIC TOXICITY TESTING OF DIFFICULT TEST CHEMICALS. OECD Environment, Health and Safety Publications Series on Testing and Assessment No. 23 https://www.oecd-ilibrary.org/docserver/0ed2f88e-en.pdf?expires=1588705829&id=id&accname=guest&checksum=C87B55DB2BE4100949CAABF98A625C98

OECD, Organisation for Economic Co-operation and Development, 2004. Test No. 218: Sediment-Water Chironomid Toxicity Using Spiked Sediment, OECD Guidelines for the Testing of Chemicals, Section 2. OECD Publishing, Paris, DOI: https://doi.org/10.1787/9789264070264-en

Park, S.Y. and Choi, J., 2017. Molecular characterization and expression analysis of P38 MAPK gene and protein in aquatic midge, *Chironomus riparius* (Diptera: Chironomidae), exposed to environmental contaminants. Archives of environmental contamination and toxicology, 72(3), pp.428-438. URL: https://link.springer.com/article/10.1007/s00244-017-0366-0

Piccinno, F., Gottschalk, F., Seeger, S. and Nowack, B., 2012. Industrial production quantities and uses of ten engineered nanomaterials in Europe and the world. Journal of Nanoparticle Research, 14(9), p.1109. URL: https://link.springer.com/article/10.1007/s11051-012-1109-9

Planello, R., Servia, M.J., Gómez-Sande, P., Herrero, O., Cobo, F. and Morcillo, G., 2015. Transcriptional responses, metabolic activity and mouthpart deformities in natural populations of *Chironomus riparius* larvae exposed to environmental pollutants. Environmental toxicology, 30(4), pp.383-395. DOI: https://doi.org/10.1002/tox.21893

Roco, M.C., 2003. Nanotechnology: convergence with modern biology and medicine. Current opinion in biotechnology, 14(3), pp.337-346. DOI: https://doi.org/10.1016/S0958-1669(03)00068-5

Rodea-Palomares, I., Boltes, K., Fernández-Pinas, F., Leganés, F., García-Calvo, E., Santiago, J. and Rosal, R., 2011. Physicochemical characterization and ecotoxicological assessment of CeO_2 nanoparticles using two aquatic microorganisms. Toxicological Sciences, 119(1), pp.135-145. DOI: https://doi.org/10.1093/toxsci/kfq311

Rogers, N.J., Franklin, N.M., Apte, S.C., Batley, G.E., Angel, B.M., Lead, J.R. and Baalousha, M., 2010. Physico-chemical behaviour and algal toxicity of nanoparticulate CeO2 in freshwater. Environmental Chemistry, 7(1), pp.50-60. DOI: https://doi.org/10.1071/EN09123

Roh, J.Y., Park, Y.K., Park, K. and Choi, J., 2010. Ecotoxicological investigation of CeO_2 and TiO_2 nanoparticles on the soil nematode *Caenorhabditis elegans* using gene expression, growth, fertility, and survival as endpoints. Environmental toxicology and pharmacology, 29(2), pp.167-172. DOI: https://doi.org/10.1016/j.etap.2009.12.003

Rohlf, F.J., 2005. TpsDig, Digitize Landmarks and Outlines. Department of Ecology and Evolution, State University of New York at Stony Brook version 2.05. http://life.bio.sunysb.edu/morph/

Rohlf, F.J., 1990. Morphometrics. Annual Review of ecology and Systematics, 21(1), pp.299-316

Savić-Zdravković, D., Milošević, D., Uluer, E. Savić-Zdravković, D., Jovanović, B., Đurđević, A., Stojković-Piperac, M., Savić, A., Vidmar, J., & Milošević, D., 2018. An environmentally relevant concentration of titanium dioxide (TiO_2) nanoparticles induces morphological changes in the mouthparts of *Chironomus tentans*. Chemosphere, 211, 489-499.

Savić-Zdravković, D., Milošević, D., Uluer, E., Duran, H., Matić, S., Stanić, S., Vidmar, J., Ščančar, J., Dikic, D. and Jovanović, B., 2020. A multiparametric approach to cerium oxide nanoparticle toxicity assessment in non-biting midges. Environ Toxicol Chem, 39: 131-140. doi: https://doi.org/10.1002/etc.4605

Salmelin, J., Vuori, K.M. and Hämäläinen, H., 2015. Inconsistency in the analysis of morphological deformities in chironomidae (Insecta: Diptera) larvae. Environmental toxicology and chemistry, 34(8), pp.1891-1898. DOI: https://doi.org/10.1002/etc.3010

Servia, M.J., Cobo, F. and González, M.A., 2000. Incidence and causes of deformities in recently hatched larvae of *Chironomus riparius* Meigen, 1804 (Diptera, Chironomidae). Archiv fur Hydrobiologie, 149(3), pp.387-401.

Sheets, H.D., 2003. IPM Suite (Integrated Morphometrics Package). Canisius College, Buffalo, NY

Stanković, J., Milošević, D., Savić-Zdraković, D., Yalçın, G., Yildiz, D., Beklioğlu, M. and Jovanović, B., 2020. Exposure to a microplastic mixture is altering the life traits and is causing deformities in the non-biting midge *Chironomus riparius* Meigen (1804). Environmental Pollution, 262, p.114248. DOI: https://doi.org/10.1016/j.envpol.2020.114248

StatSoft, Inc., 2004. STATISTICA (data analysis software system), version 7. www.statsoft.com

Tella, M., Auffan, M., Brousset, L., Morel, E., Proux, O., Chanéac, C., Angeletti, B., Pailles, C., Artells, E., Santaella, C. and Rose, J., 2015. Chronic dosing of a simulated pond ecosystem in indoor aquatic mesocosms: fate and transport of CeO_2 nanoparticles. Environmental Science: Nano, 2(6), pp.653-663. URL: https://pubs.rsc.org/--/content/articlehtml/2015/en/c5en00092k

Tomilina, I.I. and Grebenyuk, L.P., 2020. Malformations of Mouthpart Structures of *Chironomus riparius* Larvae (Diptera, Chironomidae) under the Effect of Metal-Containing Nanoparticles. Entomological Review, 100, pp.7-18. URL: https://link.springer.com/article/10.1134%2FS0013873820010029

Tomilina, I.I., Gremyachikh, V.A., Grebenyuk, L.P., Smirnov, E.A. and Golovkina, E.I., 2015. Changes in biological parameters of freshwater animals under the impact of various crystal modifications of titanium dioxide nanoparticles. Inland water biology, 8(3), pp.309-318. DOI: https://doi.org/10.1134/S1995082915030153

Vallenduuk, H.J., 2017. Chironomini larvae of western European lowlands (Diptera: Chironomidae). Keys with notes to the species. With a redescription of Glyptotendipes (Caulochironomus) nagorskayae and a first description of Glyptotendipes (Caulochironomus) kaluginae new species. Lauterbornia, 82, pp.1-216.

Wang, Y. and Nowack, B., 2018. Dynamic probabilistic material flow analysis of nano-SiO_2, nano iron oxides, nano-CeO_2, nano-Al_2O_3, and quantum dots in seven European regions. Environmental pollution, 235, pp.589-601. DOI: https://doi.org/10.1016/j.envpol.2018.01.004

Warwick, W.F. and Tisdale, N.A., 1988. Morphological deformities in Chironomus, Cryptochironomus, and Procladius larvae (Diptera: Chironomidae) from two differentially stressed sites in Tobin Lake, Saskatchewan. Canadian Journal of Fisheries and Aquatic Sciences, 45(7), pp.1123-1144. DOI: https://doi.org/10.1139/f88-136

Zelditch, M.L., Swiderski, D.L. and Sheets, H.D., 2012. Geometric morphometrics for biologists: a primer. Academic Press. DOI: https://doi.org/10.1016/B978-012778460-1/50003-X

Zhang, P., Ma, Y., Liu, S., Wang, G., Zhang, J., He, X., Zhang, J., Rui, Y. and Zhang, Z., 2017. Phytotoxicity, uptake and transformation of nano-CeO_2 in sand cultured romaine lettuce. Environmental Pollution, 220, pp.1400-1408. DOI: https://doi.org/10.1016/j.envpol.2016.10.094

Zhang, H., He, X., Zhang, Z., Zhang, P., Li, Y., Ma, Y., Kuang, Y., Zhao, Y. and Chai, Z., 2011. Nano-CeO_2 exhibits adverse effects at environmental relevant concentrations. Environmental science & technology, 45(8), pp.3725-3730. DOI: https://doi.org/10.1021/es103309n

FIGURE AND TABLE CAPTIONS

Figure 1 - Photomicrographs of *C. riparius* morphological structures with the configuration of specific landmarks that describe their morphometry: a - right larval mandible (magnified 200x); b – larval mentum (magnified 100x); c - right adult wing (magnified 10x). Leica MZ16A stereomicroscope and Leica DFC320 Digital Camera system camera.

Figure 2 - PCA and CVA analysis of the mandibles of *C. riparius* larvae exposed to CeO2 NPs. Ellipses describe the 90 % confidence interval of the mean values of each group, i.e., treatment: a - distribution of

individuals in the morphological space defined by the first and second PC axes. “Outline” graphs show specific changes in the shape of mandibles associated with each axis (scaling factor 0.01): the average shape is colored black, while the modified shape (individuals with the highest PC scores) is colored green; b - distribution of individuals in the morphological space defined by the first and second CV axes. “Outline” and “Transformation grid” graphs show specific changes in the shape of the mandibles associated with each axis (scaling factor 4): the average shape is colored black, while the modified shape (individuals with the highest CV scores) is colored green.

Figure 3 - PCA and CVA analysis of the mentums of *C. riparius* larvae exposed to CeO2 NPs. Ellipses describe the 90% confidence interval of the mean values of each group, i.e., treatment: a - distribution of individuals in the morphological space defined by the first and second PC axes. “Wireframe” and “Transformation grid” graphs show specific changes in the shape of the mentums associated with each axis (scaling factor 0.06): the average shape is colored black, while the modified shape (individuals with the highest PC scores) is colored green; b - distribution of individuals in the morphological space defined by the first and second CV axes. “Wireframe” and “Transformation grid” graphs show specific changes in the shape of the mandibles associated with each axis (scaling factor 6): the average shape is colored black, while the modified shape (individuals with the highest CV scores) is colored green.

Figure 4 - PCA and CVA analysis of right wings of *C. riparius* females exposed to CeO2 NPs. Ellipses describe the 90 % confidence interval of the mean values of each group, i.e., treatment: a - distribution of individuals in the morphological space defined by the first and second PC axes. “Outline” graphs show specific changes in the shape of the wings associated with each axis (scaling factor 0.08): the average shape is colored black, while the modified shape (individuals with the highest PC scores) is colored green; b - distribution of individuals in the morphological space defined by the first and second CV axes. “Outline” graphs show specific changes in the shape of wings associated with each axis (scaling factor 4):

average shape is colored black, while the modified shape (individuals with the highest PC scores) is colored green.

Figure 5 - CVA analysis of right wings of *C. riparius* males exposed to CeO2 NPs. Ellipses describe the 90 % confidence interval of the mean values of each group, i.e., treatment - distribution of individuals in the morphological space defined by the first and third CV axes. “Outline” and “Wireframe” graphs show specific changes in the shape of wings associated with each axis (scaling factor 6): average shape is colored black, while the modified shape (individuals with the highest PC scores) is colored green.

Table 1 - Number of selected structures photographed for analysis by geometric morphometry (∑ of photomicrographs), and the final number of photomicrographs used in the analysis for each of the concentrations

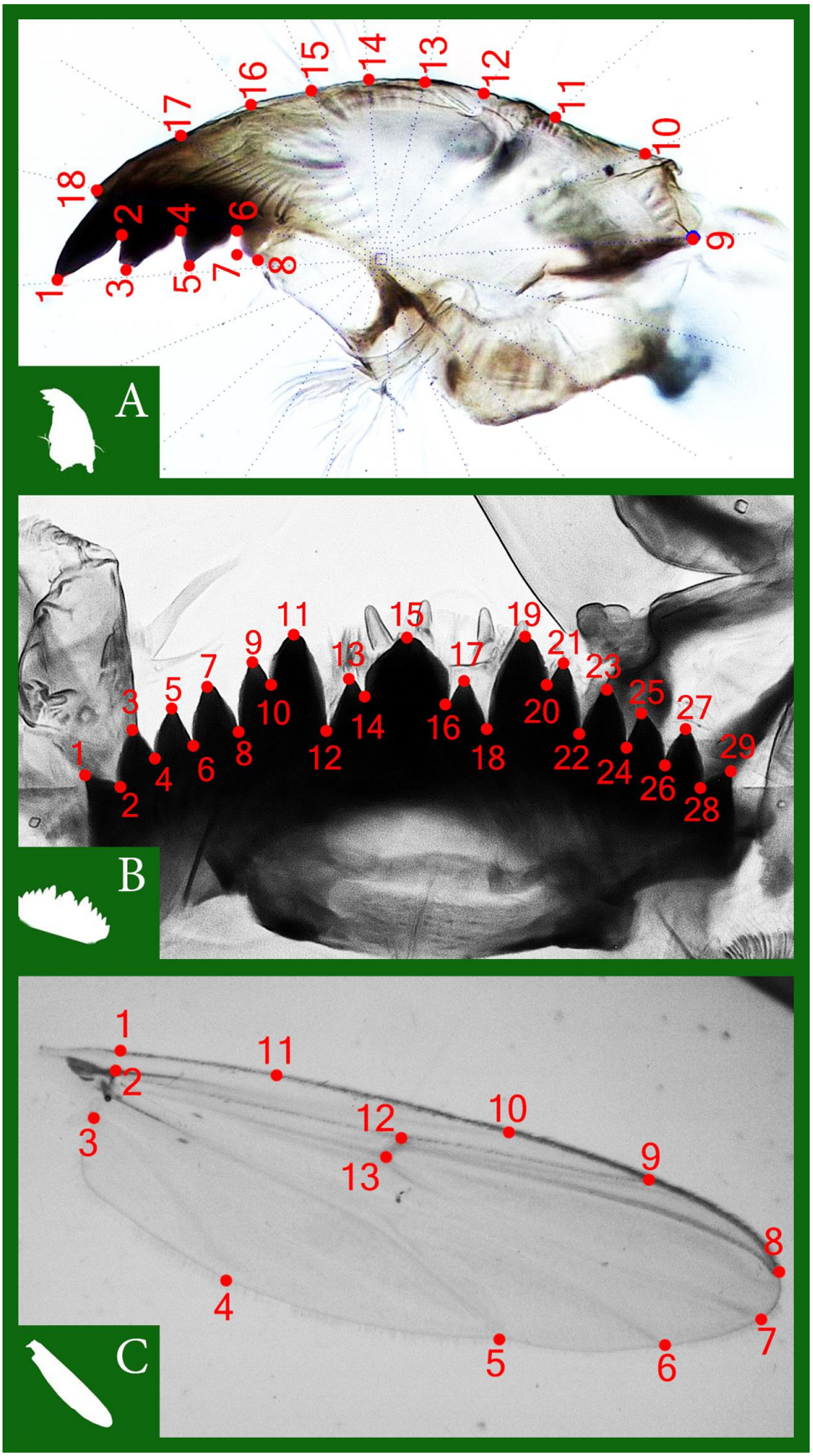
A
1
2
3
4
5
6
7
8
9
10
11
12
13
14
15
16
17
18
B
1
2
3
4
5
6
7
8
9
10
11
12
13
14
15
16
17
18
19
20
21
22
23
24
25
26
27
28
29
C
1
2
3
4
5
6
7
8
9
10
11
12
13

a

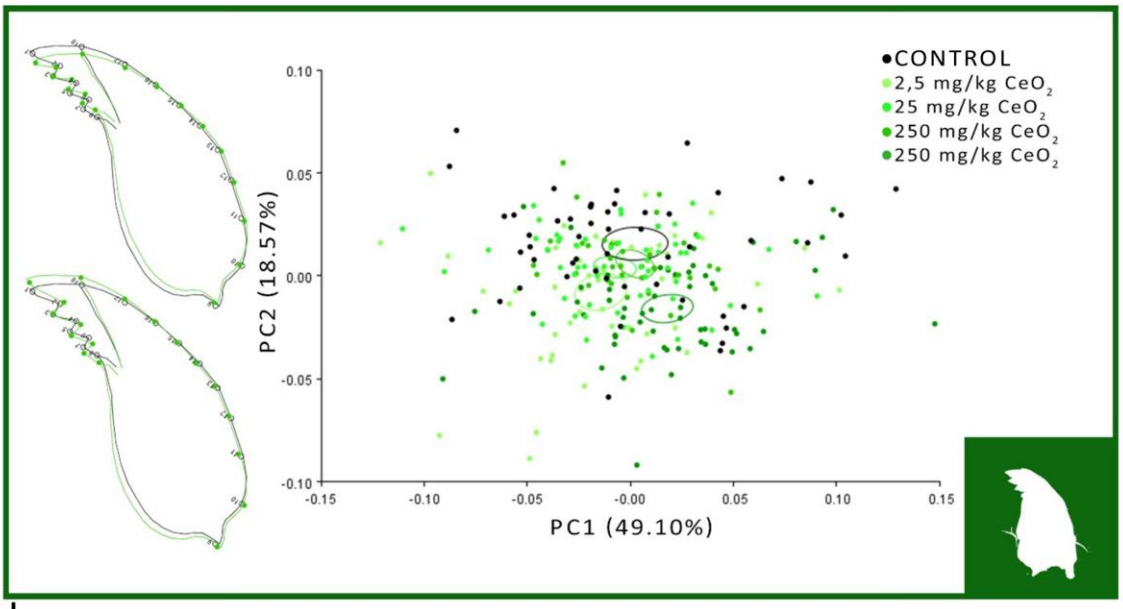
CONTROL
2,5 mg/kg CeO2
25 mg/kg CeO2
250 mg/kg CeO2
250 mg/kg CeO2
PC2 (18.57%)
PC1 (49.10%)
0.10
0.05
0.00
-0.05
-0.10
-0.15
-0.10
-0.05
-0.00
0.05
0.10
0.15

b

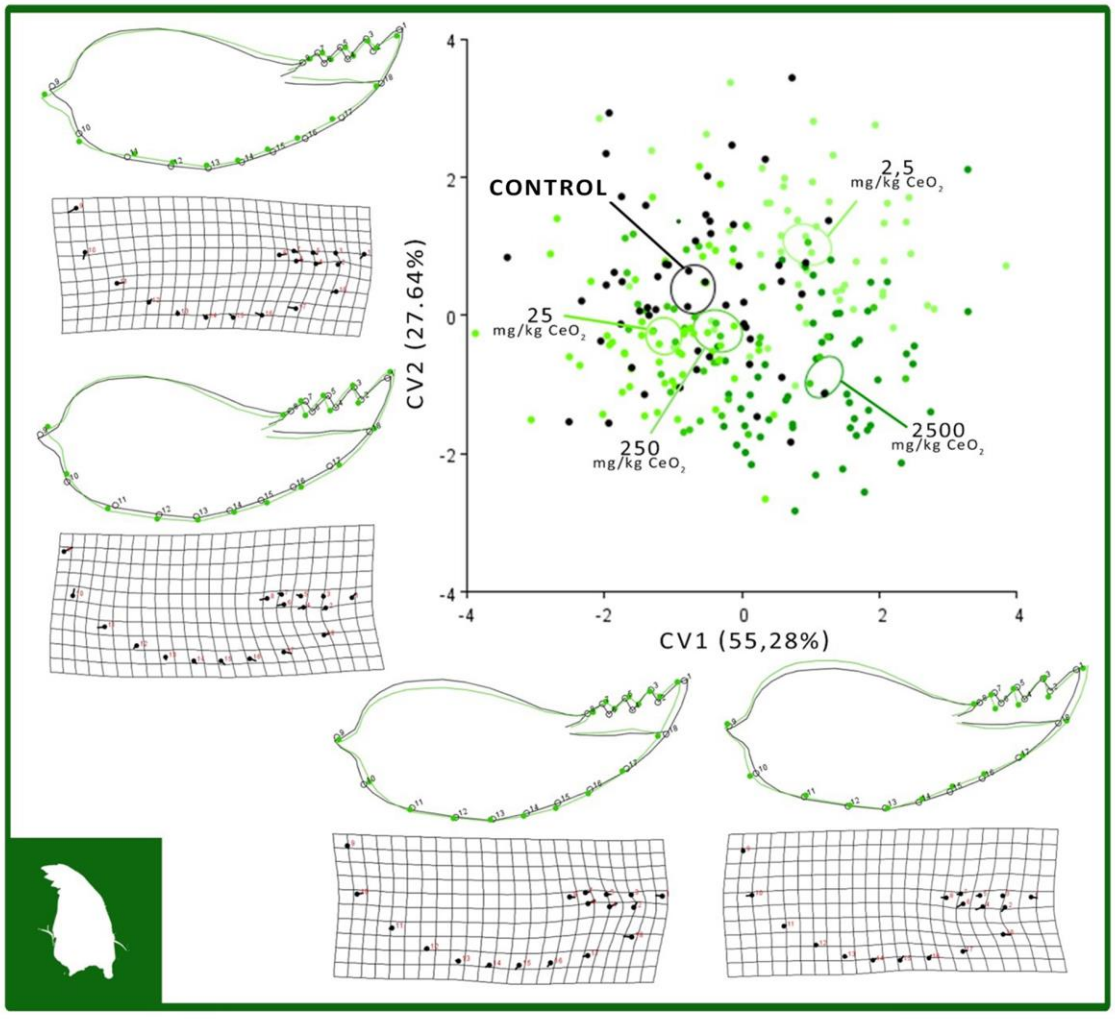
CONTROL
2,5 mg/kg CeO2
25 mg/kg CeO2
250 mg/kg CeO2
2500 mg/kg CeO2
CV2 (27.64%)
CV1 (55,28%)
4
2
0
-2
-4
-4
-2
0
2
4

a

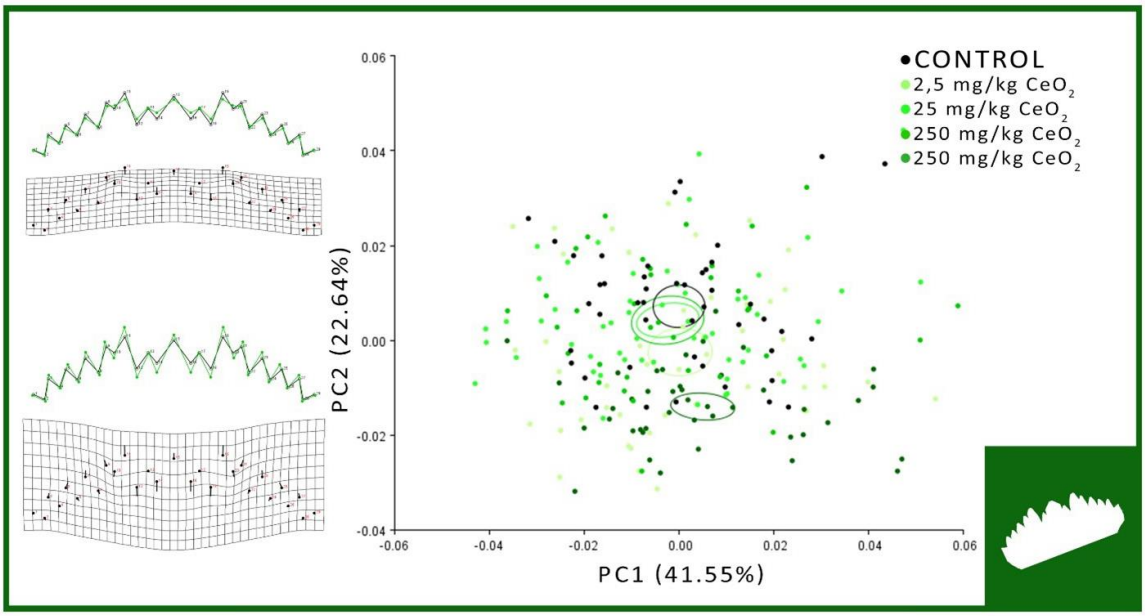
CONTROL
2,5 mg/kg CeO2
25 mg/kg CeO2
250 mg/kg CeO2
250 mg/kg CeO2
PC2 (22.64%)
PC1 (41.55%)
0.06
0.04
0.02
0.00
-0.02
-0.04
-0.06
-0.04
-0.02
0.00
0.02
0.04
0.06

b

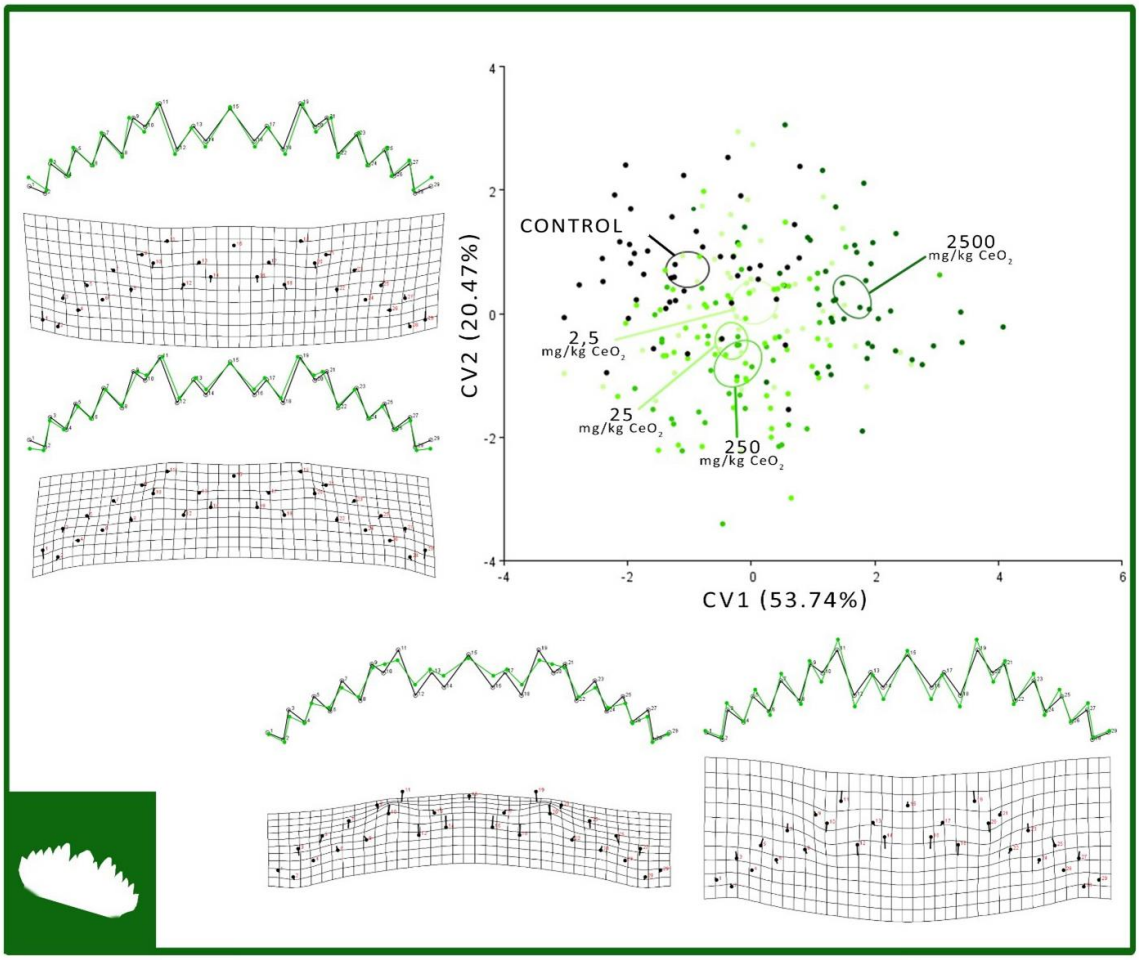
CONTROL
2500 mg/kg CeO2
2,5 mg/kg CeO2
25 mg/kg CeO2
250 mg/kg CeO2
CV2 (20.47%)
CV1 (53.74%)
4
2
0
-2
-4
-4
-2
0
2
4
6

a

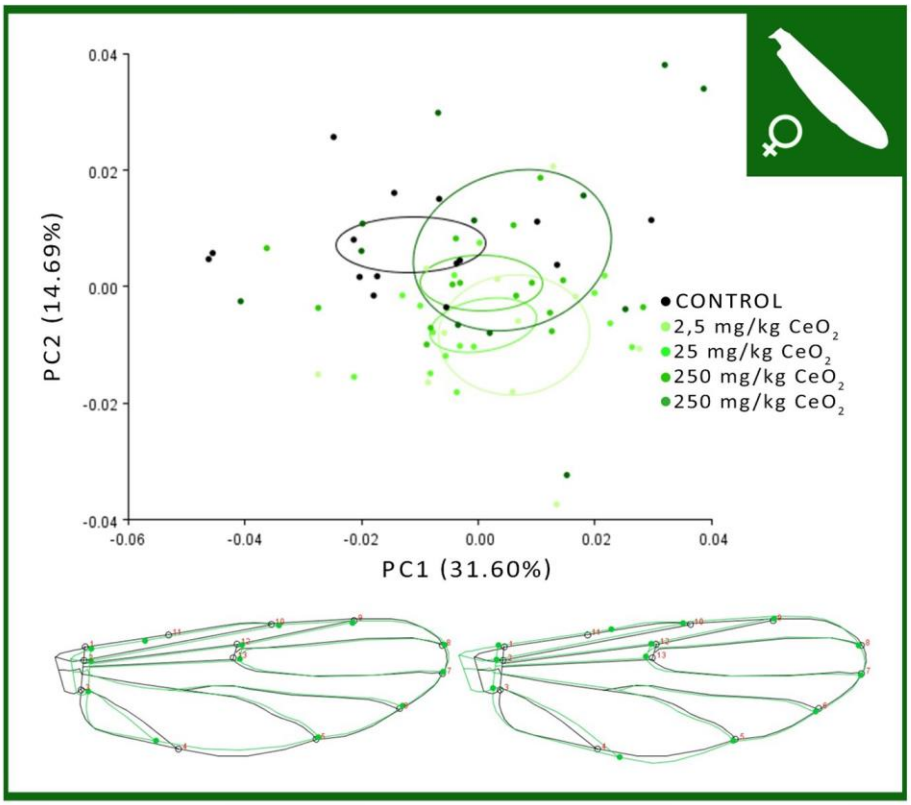
0.04
0.02
0.00
-0.02
-0.04
PC2 (14.69%)
-0.06
-0.04
-0.02
0.00
0.02
0.04
PC1 (31.60%)
CONTROL
2,5 mg/kg CeO2
25 mg/kg CeO2
250 mg/kg CeO2
250 mg/kg CeO2

b

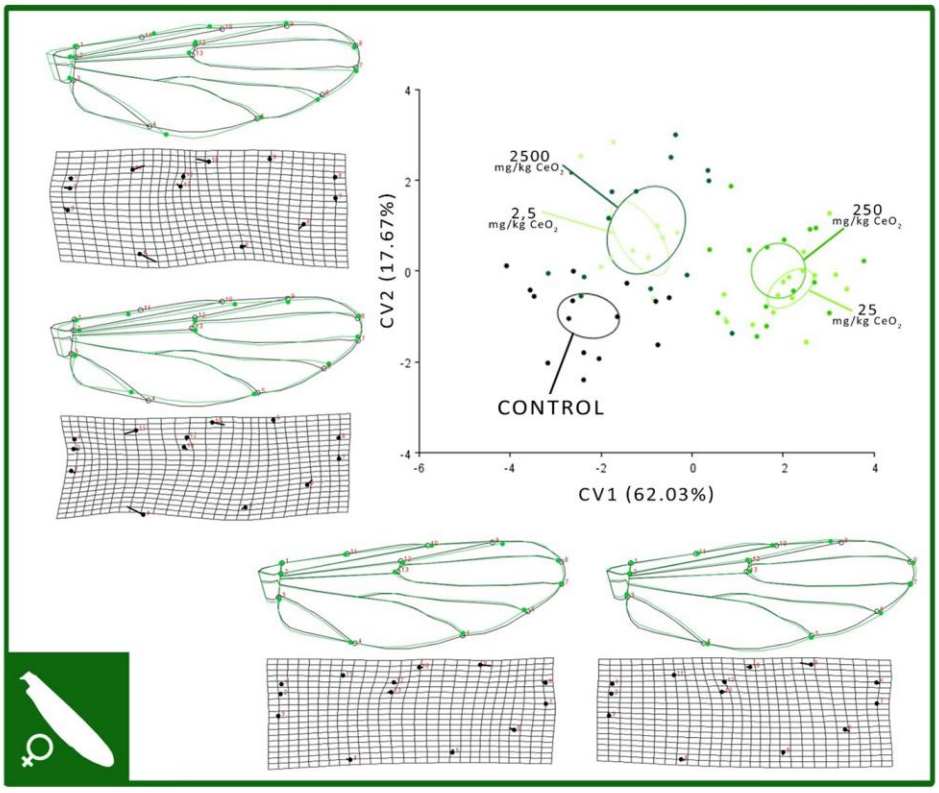
4
2
0
-2
-4
CV2 (17.67%)
-6
-4
-2
0
2
4
CV1 (62.03%)
2500 mg/kg CeO2
2,5 mg/kg CeO2
250 mg/kg CeO2
25 mg/kg CeO2
CONTROL

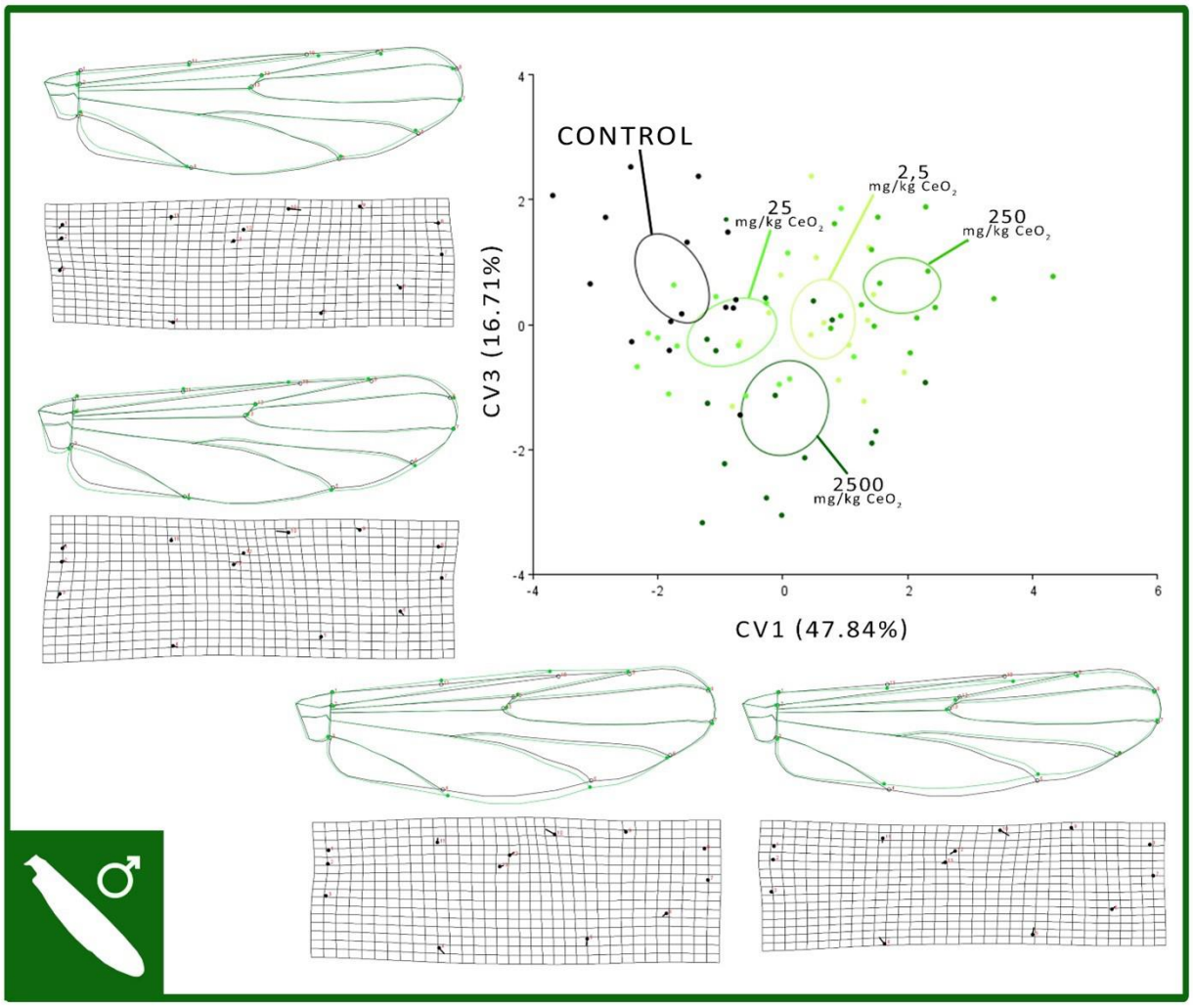
CONTROL
2,5
mg/kg CeO2
25
mg/kg CeO2
250
mg/kg CeO2
2500
mg/kg CeO2
CV3 (16.71%)
CV1 (47.84%)
4
2
0
-2
-4
-4
-2
0
2
4
6
♂

Table 2 - Number of selected structures photographed for analysis by geometric morphometry (∑ of photomicrographs), and final number of photomicrographs used in the analysis for each of the concentrations

		Larvae		Adults	
		Mandibles (right)	Mentums	Male wings (right)	Female wings (right)
Total No. of examined structures		275	275	75	75
∑ of structures excluded from geometric morphometric analysis	visible damage	5	10	0	0
	visible deformity	10	4	0	0
	Extreme values in morphoJ software	2	29	0	5
Final No. of structures included in the geometric morphometric analysis		258	232	75	70
No. of structures included in the geometric morphometric analysis **per treatment**					
treatment (mg of CeO_2 NPs per 1 kg of sediment)	2.5 CeO_2 NPs	54	49	15	12
	25 CeO_2 NPs	56	55	15	15
	250 CeO_2 NPs	39	37	15	15
	2500 CeO_2 NPs	55	44	15	13
	Control	54	47	15	15

CRediT author statement

Dimitrija Savić-Zdravković: Conceptualization, Methodology, Formal analysis, Investigation, Writing - Original Draft, Review & Editing, Visualization, Project administration; Djuradj Milošević: Conceptualization, Methodology, Validation, Formal analysis, Resources, Writing - Review & Editing, Supervision, Project administration, Funding acquisition; Jelena Conić: Validation, Investigation; Katarina Marković: Validation, Formal analysis, Investigation; Janez Ščančar: Validation, Formal analysis, Investigation; Marko Miliša: Validation, Formal analysis, Investigation; Boris Jovanović: Conceptualization, Methodology, Validation, Resources, Writing - Review & Editing, Supervision, Project administration

Declaration of interests

☒ The authors declare that they have no known competing financial interests or personal relationships that could have appeared to influence the work reported in this paper.

☐The authors declare the following financial interests/personal relationships which may be considered as potential competing interests:

Graphical abstract

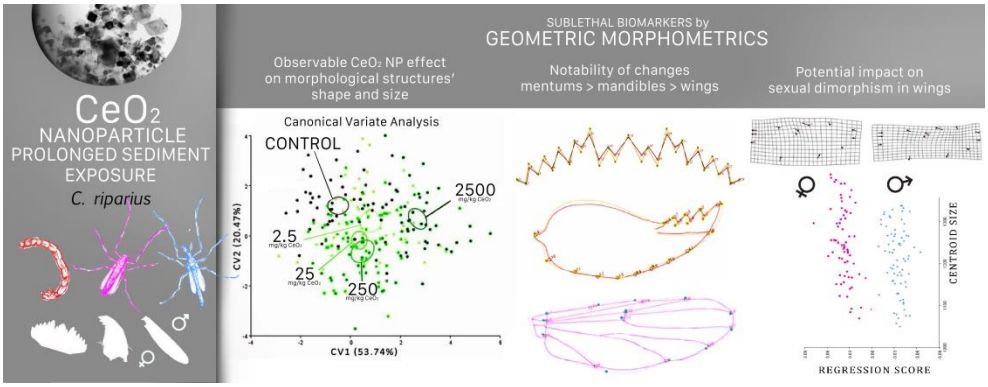

Highlights:

- 2.5 and 2500 mg of CeO_2 NPs induced morphological changes in *C. riparius*
- The prominence of changes: mentums > mandibles > female wings > male wings
- CeO_2 NPs potentially reduce *C. riparius* sexual dimorphism
- A geometric morphometric approach is suitable for assessing CeO_2 NP sublethal effects